CME ASSOCIATED WITH TRANSEQUATORIAL LOOPS AND A BALD PATCH FLARE

C. DELANNÉE[1] and G. AULANIER[2]
[1]*NASA/Goddard Space Flight Center, SOHO EAF, Mail Code 682.3, Building 26, Room G-1, Greenbelt, Maryland 20771 U.S.A., and IAS, Batiment 121, Universitée Paris XI, 91405 Orsay cedex, France*
[2]*Naval Research Laboratory, Code 7675 A, Washington, DC 20375, U.S.A., and George Masson Universtity, CSI, 4400 University Dr., Fairfax, VA 22030, U.S.A.*

(Received 16 September 1999; accepted 2 December 1999)

Abstract. We study a flare which occurred on 3 November 1997 at 10:31 UT in the vicinity of a parasitic polarity of AR 8100. Using SOHO/EIT 195 Å observations, we identify the brightening of thin transequatorial loops connecting AR 8100 and AR 8102, and dimmings located between the two active regions. Difference images highlight the presence of a loop-like structure rooted near the flare location usually called an EIT wave. The coronal magnetic field derived from potential extrapolations from a SOHO/MDI magnetogram shows that the topology is complex near the parasitic polarity. There, a 'bald patch' (defined as the locations where the magnetic field is tangent to the photosphere) is present. We conclude that the flare was a 'bald patch flare'. Moreover, the extrapolation confirms that there is a large coronal volume filled with transequatorial field lines interconnecting AR 8100 and AR 8102, and overlaying the bald patch.

We show that the dimmings are located at the footpoints of these large field lines, which can be also related to the thin bright loops observed during the flare. As this event was related to a coronal mass ejection (CME) observed by SOHO/LASCO, we propose that the observed dimmings are due to a decrease in plasma density during the opening of the transequatorial loops connecting both ARs. We propose a scenario where these large field lines are in fact pushed up by the opening of low-lying sheared field lines forming the bald patch. We finally discuss how the fast opening of these field lines can produce the brightening near the footpoints of the separatrix, observed as an 'EIT wave'.

1. Introduction

In spite of the difficulties to observe the solar atmosphere continuously from the solar surface up to several solar radii, chromospheric and low coronal phenomena have been related to coronal mass ejections observed with coronagraphs. These phenomena are mainly flares, dimmings of the low corona and EIT waves.

Many flares are called 'confined flares', because they do not lead to a CME. They have been modeled by several authors by magnetic reconnection in complex topologies (e.g., Yokoyama and Shibata, 1995; Démoulin *et al.*, 1997; Karpen *et al.*, 1998). They may indeed be triggered by an adjacent CME (as suggested by Harrison, 1986), but in some cases, the flares associated with CMEs are found to be at the origin of the CME itself (see, e.g., Innes *et al.*, 1999). Several models have been put forward to explain such 'eruptive flares'. There the flare and the CME are

Solar Physics **190:** 107–129, 1999.

both manifestations of the loss of equilibrium of a sheared magnetic field. The most common one is the 'tether-cutting' model, in which reconnection occurs in initially sheared bipolar arcades, allowing the formation of a magnetic island (or plasmoid) which is then ejected, as well as underlying closed post-flare loops (Sturrock, 1989, Mikić and Linker, 1994; Amari *et al.*, 1996a). An alternative model is the 'magnetic breakout': a complex topology allows reconnection at a null point above the central sheared arcades, removing the overlying flux and allowing the opening of the field without the necessity of plasmoid formation (Antiochos, DeVore, and Klimchuk, 1999). In both cases, the flare (i.e., reconnection) occurs after some initial shearing (i.e., growth of the configuration), allowing the partial opening of the field (i.e., the CME). In this paper we will propose a new possibility for eruptive flares, occurring in magnetic configurations having field lines tangential to the photosphere forming a 'bald patch', as defined by Titov, Priest, and Démoulin (1993).

Moreton waves are described as bright and dark semi circular threads moving on the solar surface in the Hα images (Moreton, 1961; Ramsey and Smith, 1966). The Moreton waves are associated with flares (Reigler *et al.*, 1982; Nakajima *et al.*, 1990; Kocharov *et al.*, 1994). This association led Uchida (1970) to model the Moreton wave as a shock wave produced in the corona by a release of energy associated with the flare production and propagating in the corona and in the chromosphere. The coronal counterpart of the Moreton wave is not yet demonstrated but some large-scale wave-like features have been reported in Fe XII. They have been called EIT waves or coronal Moreton waves by several authors (Thompson *et al.*, 1998, 1999; Krucker *et al.*, 1999; Torsti *et al.*, 1999).

Dimmings of the solar corona associated with CMEs are reported in soft X-rays (Rust and Hildner, 1976; Hudson, 1997; Sterling and Hudson, 1997; Gopalswamy and Hanaoka, 1998) and are sometimes associated with large transequatorial loops (Khan and Hudson, 1999; Maia *et al.*, 1999; Wills-Davey and Thompson, 1999). They develop on a time-scale faster than an hour and can last for several days. The development of the dimmings is faster than the typical time-scale of the cooling of the corona. So, they can be interpreted as a density decrease as the ejection occurs (Hudson, Acton, and Freeland, 1996). The dimmings are also observed in EUV (Dere *et al.*, 1997; Bumba, Garcia, and Jordan, 1998; Gopalswamy *et al.*, 1998; Thompson *et al.*, 1998; Delannée, Delaboudinière, and Lamy, 2000). In some cases, the presence of dimmings at several wavelengths in the EUV at the same time re-enforces the hypothesis that they correspond to density decrease (Thompson *et al.*, 1998).

The corresponding CMEs are observed in the coronagraphs field of view. They present a bright leading loop followed, in some cases, by a cavity and finally in some more few cases, followed by the core of the remaining of an erupting prominence (Delannée, Delaboudinière, and Lamy, 2000). The angular width of the CMEs are found to be 40 degree on average over 1209 CMEs observed with the Solar Maximum Mission (Hundhausen, 1993).

We present here the study of the low coronal signatures on the solar disc of a CME compared with the extrapolation of the magnetic field lines of the region involved in the ejection. A scenario of the processes of the ejection is proposed and discussed. In Section 2, the methods of study are described: observations and extrapolations. In Section 3, the observed structures, appearing during and after the ejection, are described and compared with the extrapolated magnetic field lines. In Section 4, the possibility of a bald patch flare as the source of the ejection is discussed. In Section 5, the processes involved in the ejection are presented and related to the observed features (flare, dimmings, EIT wave, transequatorial loops). In Section 6, we discuss several issues raised in the paper, and we point out that magnetohydrodynamic simulations are needed to validate our interpretation of the event. Section 7 finally gives a summary of the results obtained in the paper.

2. The Tools for the Study

In this section, we present the observations used in this study. The instruments on board the Solar and Heliospheric Observatory are used to obtain the observations of the corona on the solar disc and above the solar limb, and to obtain the photospheric magnetic field. The extrapolation of this magnetogram is used to obtain the magnetic field in the corona.

2.1. Coronal observations from EIT/LASCO

The Extreme ultraviolet Imaging Telescope (EIT, Delaboudinière *et al.,* 1995) uses a filter centered on 195 Å to observe the whole Sun in the Fe XII emission line every 17 min. The pixels are binned 2 by 2 to permit a faster acquisition of the data which leads to a pixel size of 5.24″. The Fe XII line is formed at a temperature of about 1.5×10^6 K at coronal densities. The different features in the corona appear in a very wide range of intensities. In this paper, the logarithm of the intensities is displayed on the images to get a better contrast. The properties of the corona in this line permit following the development of the mass loss on the solar surface and above the limb (Dere *et al.,* 1997; Thompson *et al.,* 1998; Delannée, Delaboudinière, and Lamy, 2000). However, the signature of the CME initiation in this line is very faint and some processing is needed to reveal it such as the difference of the intensities of the images with a preceding one. In this paper, the images are first coaligned to the magnetogram then de-rotated to the time of the magnetogram used in the study. Finally, the difference is applied between the images and an image obtained at 10:22 UT, i.e., prior to the first image of the ejection.

The event studied here is found to be related to a CME (Delannée, Delaboudinière, and Lamy, 2000) observed with the Large Angle and Spectrometric Coronagraph (LASCO, Brueckner *et al.,* 1995) C2 in white light using a filter centered on 5800 ± 600 Å. The LASCO C2 field of view covers $2-6\ R_\odot$. The spatial resolution

is 11.4″. One image of LASCO C1 in Fe XIV is used to reveal the coronal loops very close to the limb. The LASCO C1 field of view covers 1.1–3 $R_\odot$. The spatial resolution is 3″ per pixel. The spectral resolution is very narrow due to the use of a Fabry–Pérot. The wavelength band pass used is 5303 ± 0.63 Å.

2.2. PHOTOSPHERIC MAGNETIC FIELD OBSERVED BY MDI

The Michelson Doppler Imager (MDI, Scherrer *et al.*, 1995) provided the magnetogram used in this study. The Zeeman splitting of the photospheric Ni I absorption line at 6767.8 Å is determined by the difference between the Doppler shifts calculated from the filtergram components and the circularly polarized light. The per-pixel measurement uncertainty for a 2 min measurement is equivalent to 10 gauss. The pixel size is 1.97″.

As only the photospheric magnetic field can be determined, the MDI field of view is the whole Sun plus an annulus about 10″ wide above the limb. The remaining pixels located between this disc and the edges of the square field of the CCD have non numerical quantities. For the purpose of magnetic field extrapolation, the part of the magnetogram located above the solar disc is set to 0 gauss.

2.3. CO-ALIGNMENT OF THE DATA

The key of the understanding of the quiet and dynamic structures in the solar corona is knowing the magnetic field, unfortunately no clean measurements are available in this layer of the Sun. However, the photospheric magnetograms can give some hints about it, combined with theoretical magnetic field extrapolations. The calculated field lines can then be compared to observed UV loops, providing that a correct co-alignement was done between the magnetogram and the UV observations. This becomes crucial when dealing with small scale events or resolved features, such as flares related to parasitic polarities.

All the EIT images of the studied event (starting at 10:31 UT) are co-aligned to the MDI image which was obtained closest in time (i.e., at 14:24 UT) according to their pointing and pixel sizes. We then finally consider only a field of view of $1641'' \times 1522''$ which means 1173×1088 Mm^2 for the EIT as well as the MDI data (see Figure 1). Even if this study involves a large scale area of the Sun, we present in Figure 2 a close-up of AR 8100 observed at 07:11 UT, in order to avoid the saturation effects during the flare.

2.4. POTENTIAL MAGNETIC FIELD EXTRAPOLATION METHOD

The temperature range of the plasma in some loops, as well as several other quantities such as low density or filling factor, often makes them difficult to be identified in observations. One natural way to bring complementary results to the morphology of the loops observed by EIT is to make magnetic field extrapolations.

As shown on Figure 1, a very large portion of the Sun is involved in the studied event. On such scales, sphericity plays a role on the magnetic field structuring of the corona. Moreover, it leads to extending the true size of the solar photosphere compared to what is directly observed. As a consequence, a suitable magnetic field extrapolation should be performed in spherical coordinates. Nevertheless, we restrict ourselves to the Cartesian geometry approximation. We then assume the photosphere to be a plane, thus neglecting all curvature effects. Such a coarse assumption can be disputed (see Section 6), but we will show that if it indeed slightly modifies the shape of the field lines, it is not very important with respect to the field connectivity and topology, as long as regions which are not too far from the limb are not considered: Gary and Hagyard (1990) and Démoulin *et al.* (1997) give a 2% error for the magnetogram pixel size for regions located at 40 degrees off the disc center.

We used the linear force-free field *lfff* extrapolation code described in Démoulin *et al.* (1997), which solves the equation $\nabla \times \mathbf{B} = \alpha \mathbf{B}$, in Cartesian geometry, for α = constant. Because of the limitations on the maximum value of α which can be used for such a large region, and as the field is known to be nearly potential at high heights rather than sheared (see Schmieder *et al.,* 1996), we use the potential approximation, i.e. $\nabla \times \mathbf{B} = \mathbf{0}$.

Let the photospheric 'plane' be (x,y) and the altitude be z. In a first step, the SOHO/MDI magnetogram (which is $1641'' \times 1522''$) is put at the center of a larger region $\Delta x \times \Delta y$, where $\Delta x = \Delta y = 1660''$. In this square, the field outside the considered magnetogram is set to $B = 0$. The observed line of sight component of the magnetic field is assumed to be vertical, i.e. perpendicular to (x, y). This gives the (x, y) boundary conditions at $z = 0$ for the extrapolations. The vertical component of the magnetic field is then decomposed in a series of Fourier harmonics, using a Fast Fourier Transform on 256×256 points. The latter imposes periodic boundary conditions on the sides of the computational domain (Alissandrakis, 1981). The three components of the field, as well as their different values with z, are then derived from the potential field equation. The magnetic field is computed at every height from $z = 0''$ to $350''$. The result is finally stored in a box of $129 \times 129 \times 61$ mesh points. The cells are uniformly distributed in (x, y), giving a horizontal cell size of $\delta xy = 12.87''$. The mesh is non uniform in z, going from $\delta z = 1''$ to $17''$, from the bottom to the top of the box.

3. The Development of the CME in the Solar Corona

We describe here the previous studies of this ejection. The temporal and spatial relation between the different structures, flare, dimmings, large-scale loops, are described in detail and compared to the extrapolated magnetic field lines.

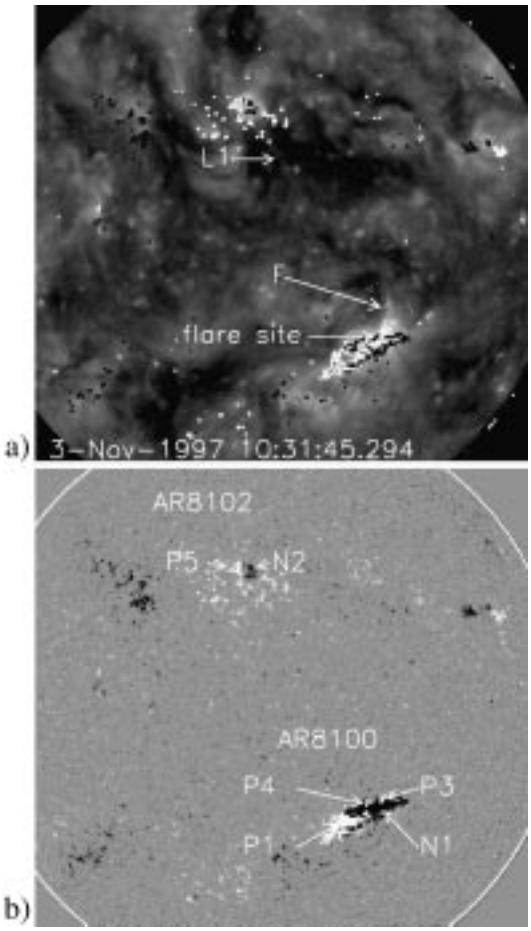

Figure 1. (a) The first SOHO/EIT 195 Å image of the CME event, obtained at 10:31 UT. (b) The SOHO/MDI magnetogram obtained at 14:24 UT. The main polarities of AR8100 are called N1 (negative polarity) and P1 (positive polarity) and the parasitic polarities are called P3 and P4.

3.1. SUMMARY OF PREVIOUS STUDIES

AR 8100 is found to be at the origin of 8 CMEs emitted during the period from 1 to 6 November 1997 (Delannée, Delaboudinière, and Lamy, 2000). During this period, due to the rotation of the Sun, the active region is moving from the central meridian to the limb. All the events appear to be very similar but a detailed study of each of them was not done in this previous paper.

Particular attention was paid to the 6 November 1997 CME by Maia *et al.* (1999). This CME is produced near AR 8100 when it is near the limb. An X9 flare is detected by the GOES satellite. The related CME has a velocity of about 1700 km s^{-1}. The authors conclude that the sources of the radio emission of this event are due to the interaction of some coronal loops, and are likely to be

signatures of magnetic reconnection. This primary energy release seems to occur between the loop connecting two polarities inside the active region and a transequatorial loop connecting AR 8100 to AR 8102 (N30W35). The CME seems to lift off just after the interaction. Then some other interactions occur between several loops inside AR 8102.

Now we will describe one of these 8 events. On 3 November 1997, AR 8100 is located at S19 W19 and AR 8102 at N30 E07. On 3 November 1997 3 CMEs occur in AR 8100, the two first ones are difficult to study in detail because of the very low differences in intensity between images prior the events and the ones during the event. We choose to focus on the ejection which occurred on 3 November 1997 at 10:31 UT for which the images show some clear structures related to this events. The magnetogram of the whole region is nearly centered on the central meridian so that both active regions are not too far from the disc center. The signature of the CME at 195 Å is composed of three parts, a flare, a dimming and a bright front usually called an EIT wave.

3.2. THE FLARE, THE BRIGHT FRONT AND THE CORONAL DIMMINGS

The MDI magnetogram obtained at 14:24 UT shows that AR 8100 presents a complex photospheric magnetic field pattern. Two main polarities are present, P1 and N1 (see Figure (1b)). A sunspot is at the location of the positive polarity. The negative polarity is quite elongated. Two parasitic positive polarities (P3 and P4) lie at the northern edge of N1. It is noteworthy that of the 8 flares related to the 8 CMEs produced during the 1–6 November 1997 period, only one is related to the P4 polarity and 6 are related to the P3 polarity. On 6 November 1997 the involved polarity is too difficult to identify on the magnetogram, due to the fact that AR 8100 is located near the limb.

In the present studied event, a flare is present in the first image of the event (see Figure 1(a), at 10:31 UT). The superposition of the magnetogram with the 195 Å image shows that the flare is very close to the neutral line formed between the main negative polarity (N1) and the positive parasitic polarity (P3) in AR 8100 (see Figure 1(b)). The northern part of the flare has a shape of a flame (see the feature F on Figure 1(a)).

On the same first image of the event, a bright front appears in the shape of a loop located in the northern region of AR 8100. The difference image reveals that a dimming is located between the bright front and AR 8100 (see Figure 3(a)). The bright front lies very close to the northern edge of F.

On the following 195 Å difference image (at 10:48 UT, see Figure 3(b)) the bright front is still visible at the same location as in the previous image (at 10:31 UT, see Figure 3(a)). One has to keep in mind the possibility that this bright front observed at 10:48 UT may be a second EIT wave which was produced later. This would be a surprising coincidence that two different waves in propagation would be observed exactly at the same location for two different times, but it might be

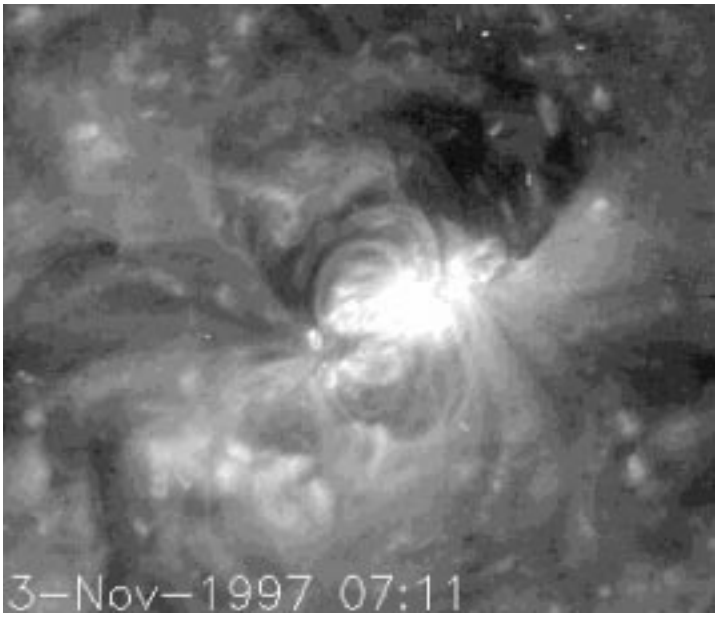

Figure 2. SOHO/EIT 195 Å image of a close-up on AR 8100 before the flare.

possible. However, no other flare is observed in 195 Å in the active region or near the active region, which could produce another wave. Moreover, no other flare is reported on the Sun between 10:29 UT and 12:23 UT on 3 November 1997 (*Solar-Geophysical Data* report). So, we cannot find any secondary energetic event which could have produced a second bright front. As a consequence, the observed EIT wave is very likely to be a stationary feature in this event! The dimming has expanded on the solar surface. The one which was observed on the image at 10:31 UT still remains and two others developed, lying between 3 features which appeared brighter than in the previous image (see features L1, L2, L3 in Figure 3(b), and next section for description). On the final difference image at 11:07 UT the dimmings start to fade, and the bright loops (L1, L2, L3) as well as the bright front have disappeared (cf., Figure 3(c)).

3.3. THE BRIGHTENING OF LARGE-SCALE TRANSEQUATORIAL LOOPS

A large loop is present on the image at 10:31 UT (L1, see Figure 3(a)). This loop seems to connect AR 8102 to AR 8100. It is observed as a bright feature in the difference image at 10:48 UT. Two others brightenings, one in the north (L2) and one in the south (L3), are present in this image. They not only delimit the edges of the dimmings, but they are also observed as elongated features which seem to link AR 8100 and AR 8102. So, we believe that they are transequatorial loops connecting the two active regions. They brighten, as well as L1 does, when the ejection occurs.

3.4. COMPARISON WITH COMPUTED FIELD LINES CONNECTING BOTH ARS

The magnetic field lines computed through the potential extrapolation can be related to the large scale loops observed by EIT (see Figure 4(c)). L1 overlays the field line marked at the head of the arrow. The field lines located NW show a tendency to go toward the west limb when they emerge from AR 8102 and before they join AR 8100, as L2 does. The SE field lines tend to go toward the east limb when they emerge from AR 8100 and before they join AR 8102, as L3 does. However, no field lines were clearly found to match the location of L2 and L3 in the extrapolation. The differences in shape of the observed and the computed loops may be due to the limited height of the range of computation, but more likely to the Cartesian coordinates used in the extrapolation. L2 and L3 may be related to some field lines coming out of the computational box (see Figure 4(c)), which then probably form very high loops. Spherical extrapolations would lead to a slightly different distribution of the magnetic field with height. We believe that these two effects may explain the discrepancy between the observed loops (L2 and L3) and the computed field lines.

The projection onto the plane of the sky off the limb of the extrapolation and the comparison with the observation support our results. The LASCO C1 image in Fe XIV line at 11:05 UT on 8 November 1997 is superposed with the image of the difference of EIT Fe XII images at 10:59 UT and at 11:15 UT, both on 8 November 1997 (see Figure 5(b)). At this time, AR 8102 has nearly disappeared and AR 8100 is very close to the limb. Large-scale loops connecting the two active regions are both present in the observations and in the computation.

3.5. LOOPS IN THE ACTIVE REGIONS

The magnetic field lines connecting the main polarities inside both active regions do not clearly match the observed loops. The reason may be the use of the potential approximation and the cartesian coordinates. However, doing extrapolations on a smaller portion of the magnetogram centered on AR 8100 and comparing the computed field lines with observed loops, we have estimated the shear to be $\alpha = 0.4 \times 10^{-2}$ Mm^{-1}. This value justifies the large-scale potential approximation, as it is rather low compared with typical sheared active regions for which 0.8×10^{-2} Mm$^{-1} \leq |\alpha| \leq 1.9 \times 10^{-2}$ Mm^{-1} (Aulanier *et al.*, 1998b).

Above the limb, the loops inside AR 8100 are well correlated to the computed field lines (see Figure 5), especially the southern loops which seem very sheared despite the fact that they are nearly potential. This sample shows how the projection effects can affect our understanding of the shape and of the physics of the corona. AR 8102 is quite far from the limb on 8 November 1997 (N30 W58). AR 8099 is located behind the limb (N30 W126, which means 36 deg behind the west limb) but almost as far from the limb as AR 8102 is. The observation above the limb at N30 may then represent the loops of the 2 active regions, so the projection on the

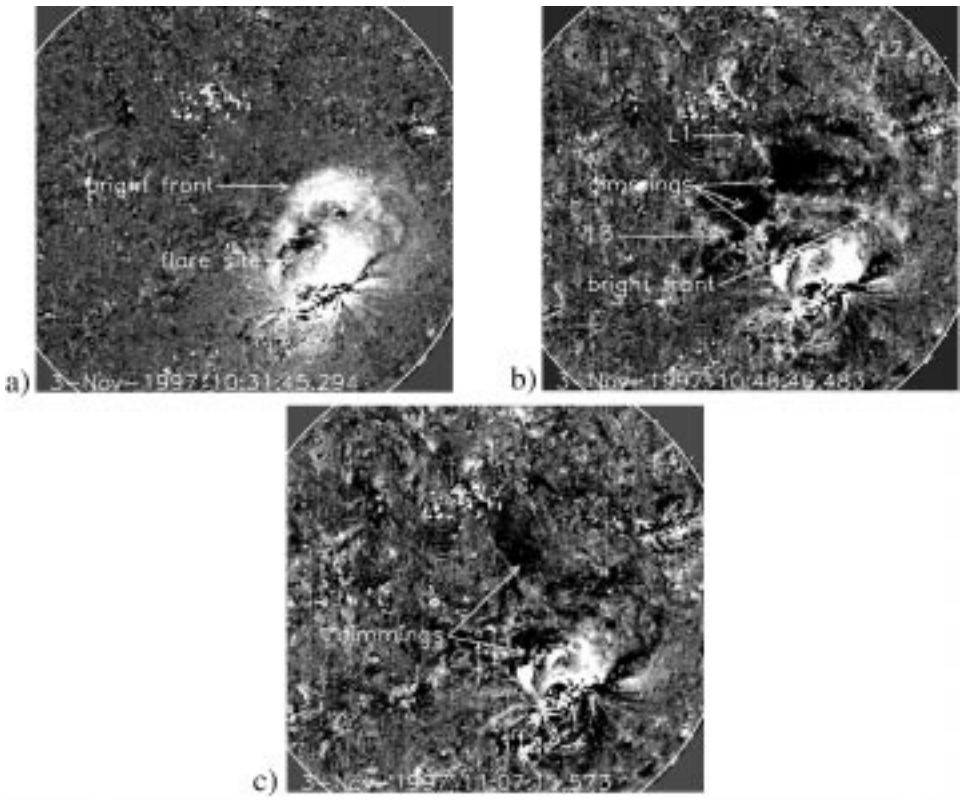

Figure 3. SOHO/EIT 195 Å observations of the development of the CME, displayed by images of difference of the Fe XII observation at a given time with the pre-event image obtained at 10:22 UT, and overlaid with the SOHO/MDI magnetogram.

limb of the extrapolated northern magnetic field lines of AR 8102 (in Figure 5(a)) can be misleading and does not represent all the observed loops.

4. A 'Bald Patch Flare' as a Source of the CME?

In this section we study the complex magnetic topology derived from the potential extrapolation in the vicinity of the flare. We then discuss the possibilities of reconnection as well as partial opening of the field in this particular topology, in order to apply it to the studied event.

4.1. THE MAGNETIC TOPOLOGY AROUND THE PARASITIC POLARITY

A study of the field line connectivity near the parasitic polarities on the northern border of N1 shows that some field lines are tangential to the photosphere on some portions of the local closed inversion lines around P3 and P4. These locations have

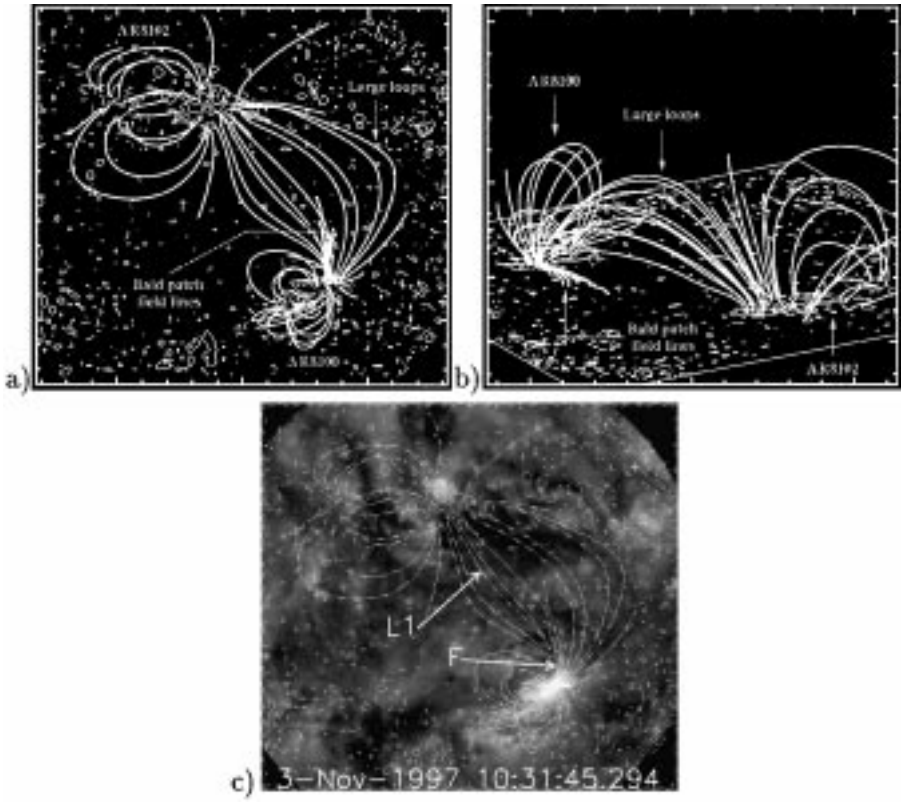

Figure 4. Comparison of the large-scale potential extrapolation with the observations. (a) The projection from the top of the computed magnetic field lines. (b) A perspective visualization of the same field lines. (c) The overlay of the extrapolated field lines and the 195 Å image at 10:31 UT.

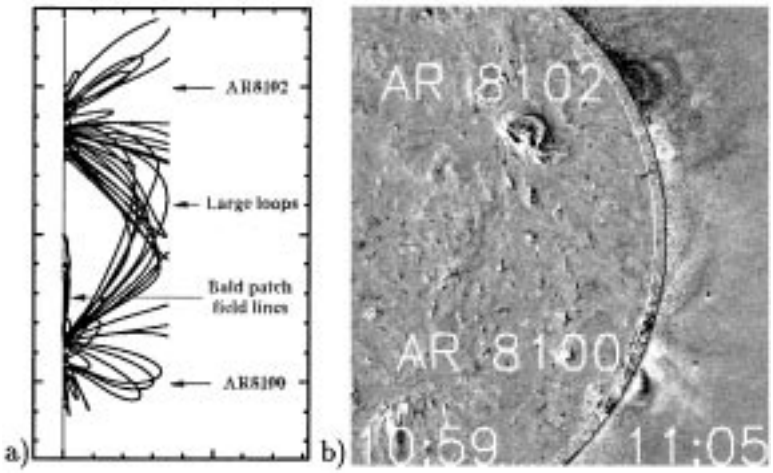

Figure 5. (a) Projection of the extrapolated field lines, as they would be observed on the west limb. (b) Fe XIV LASCO C1 image and 195 Å EIT image obtained on 8 November 1997, when AR 8100 was located near the limb. The computed transequatorial field lines can be related to observed loops.

been named 'bald patches' (or BP) by Titov, Priest, and Démoulin (1993). In this paper, the BPs are computed at the altitude $z = 0$ where the vertical field component $B_z = 0$. We use the criterion for a BP derived from the general expression for the curvature of a field line (Aulanier and Démoulin, 1998):

$$B_x \frac{\partial B_z}{\partial x} + B_y \frac{\partial B_z}{\partial y} > 0 \, . \tag{1}$$

Here we will focus on the BP associated with P3 only, as the flare studied in this paper occurred near P3. However most of what follows is still valid for P4, near which one other flare associated with a CME was also observed (mentioned in Section 3.2).

The BP topology has been extensively described by several authors (Low and Wolfson, 1988; Titov, Priest and Démoulin, 1993; Bungey, Titov and Priest, 1996; Titov and Démoulin, 1999). Nevertheless we give here a short summary, applying it to the BP of P3. All the field lines anchored in the curved line of the BP define the separatrix surface. It consists of two closed 'lobes' joined at the BP. They define three different topological regions. The first one is the overlaying arcade system, surrounding the separatrix, and the two other ones are smaller arcades confined below the separatrix and on each side of the BP. In our case the separatrix is very asymmetric: the maximal length and height of the northern lobe are 320″ and 20″ respectively, while they are 40″ and 5″ respectively for the southern one (see Figure 6). This shows how flat the separatrix surface is, and how it is extended in the north toward AR 8102.

Figure 4(c) shows that the 'F' feature associated with the flare and observed at 10:31 UT (described in Section 3.2) is well correlated with some field lines forming the BP separatrix. This suggests that some heating occurs in the BP separatrix, i.e., that energy is released there.

4.2. Reconnection in a 'bald patch'

Current sheets are known to be formed in a BP separatrix when photospheric footpoint motions are applied in their vicinity (Low and Wolfson, 1988; Vekstein and Priest, 1991; Billinghurst, Craig, and Sneyd, 1993). This naturally leads to a tearing instability, triggering magnetic reconnection or diffusion. Seehafer (1986) and Bungey, Titov, and Priest (1996) have proposed that this process could lead to a flare. However, strong energy release in BP topology is still under debate, because of following reasons: (i) the weak line tying at the BP, broadening the current sheet to a thick current layer (shown by Karpen, Antiochos, and DeVore, 1990, 1991), and (ii) the absence of a null point, leading to a slow rate of reconnection and hence to weak energy release (discussed by Antiochos, 1987).

Concerning (i), the simulations of Karpen *et al.* (1998) were done with a chromospheric-like atmosphere (10^{11} cm$^{-3} \leq n \leq 10^{15}$ cm^{-3}). In their simulations, some of the dipped field lines were slowly rising in altitude, when shearing motions were

applied. This also prevented the formation of a very thin current layer. But in a dense photospheric layer (Vernazza, Avrett, and Loeser, 1981, give $n \simeq 10^{17}$ cm^{-3} at $\tau_{500} \simeq 1$), this tendency may not be so important. In a first order approximation, neglecting the magnetic pressure term, the only force that will make the dips rise in altitude is the curvature term of the Lorentz force:

$$\mathbf{F}(\text{curv}) = \frac{B^2}{\mu R}\mathbf{u}_z \ , \tag{2}$$

where R is the curvature radius of the field line at the BP and $\mathbf{u}_z$ is the unit vector normal to the photosphere. The dense plasma will then be lifted in the BP only if $\mathbf{F}(\text{curv}) > \rho g_\odot \mathbf{u}_z$, i.e.,

$$R < R_c = \frac{B^2}{\mu \rho g_\odot} \ . \tag{3}$$

For the BP modeled in the present study, the extrapolation gives 20 G $< B <$ 40 G. Considering a typical mean field amplitude of 30 G, one finds typical critical radii of

$$R_c(\text{high chromosphere}) = 160 \text{ Mm} \ , \tag{4}$$

$$R_c(\text{low chromosphere}) = 16 \text{ km} \ , \tag{5}$$

$$R_c(\text{photosphere}) = 160 \text{ m} \ . \tag{6}$$

This crude approximation shows that the field is indeed not line-tied in the high chromosphere above a BP (in accordance with Karpen *et al.*), but that a BP needs to be very stretched up to lift photospheric plasma. Considering an initially rather flat field line (with large value of R) which then becomes stretched up by some evolution (so that R decreases). The very small value of R_c(photosphere) implies that very strong currents, as well as several plasma instabilities, will occur in this field line, even before $R < R_c$(photosphere). So, line tying may not be such a problem for strong current formation in BPs.

The problem (ii) has been studied by several authors. Low and Wolfson (1988) have proposed that a vertical current sheet may appear above a BP. The simulations of Billinghurst, Craig, and Sneyd (1993) have shown that it is hard to get such a vertical sheet, except when very large shearing motions are applied on each side of the two lobes forming the separatrix. Low and Wolfson (1988), as well as Aly and Amari (1997) have shown that such a vertical current sheet formation necessarily implies the appearance of a null point in the current sheet. One can then expect that under specific footpoint motions, a vertical current sheet can be formed above the BP, and that it forms a null point, at which reconnection naturally takes place.

It is finally worth noticing that BPs computed from extrapolations have been related to observed weak flares (see Seehafer and Staude, 1980; Seehafer, 1985; Aulanier *et al.*, 1998a). Assuming that the extrapolations are relevant, these results

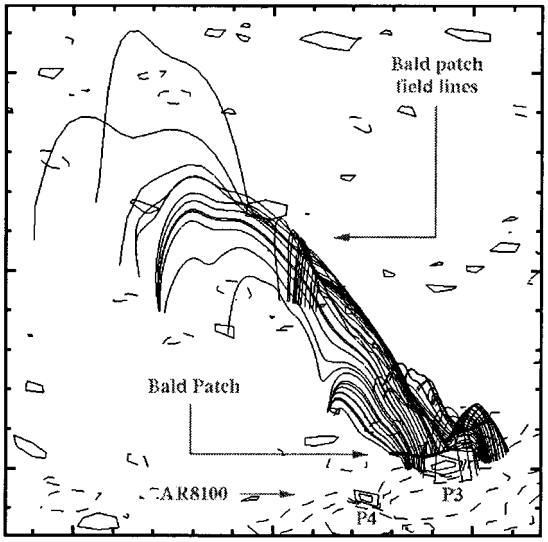

Figure 6. Perspective view of the field lines forming the separatrix associated with the bald patch. A factor $\times 4$ vertical stretching is applied in order to get a better view of these very flat field lines.

show that despite of all the controversies about vertical current sheet formation and line tying in BPs, energy can indeed be released in the so-called 'bald patch flares'.

4.3. OPENING THE FIELD IN A SHEARED 'BALD PATCH'

Let us simplify the computed magnetic configuration shown in Figure 6: we consider a 2.5-D symmetric BP topology as initial condition (see Figure 7(a)). We then describe the expected evolution of this configuration, however we emphasize here that this is only a scenario, and that it needs to be confirmed through MHD simulations.

When large photospheric shearing motions are applied to the field lines anchored in the photosphere around the BP, one expects that the 'sheared configuration' inflates, eventually forming a vertical current sheet (see Figure 7(b)). The ideal MHD evolution with a continuous shearing is expected to open the field partially through a quasi-static evolution (see Figure 7(c)), by analogy with the ideal shearing of 2.5-D bipolar arcades (see Mikić and Linker, 1994; Amari *et al.*, 1996a). However, it is very likely that during a resistive evolution a null point will appear in the forming vertical current sheet, eventually leading to reconnection between two adjacent sheared field lines (see Figure 7(d)).

The critical issue in the triggering of a CME is the opening of the field. By analogy with the 'tether cutting' model (Sturrock, 1989; Mikić and Linker, 1994; Amari *et al.*, 1996a), the resistive evolution of the sheared BP may lead to the 'partially open state' shown in Figure 7(e). This will only be possible if the evolution from Figure 7(b–e) is energetically favorable, i.e., if

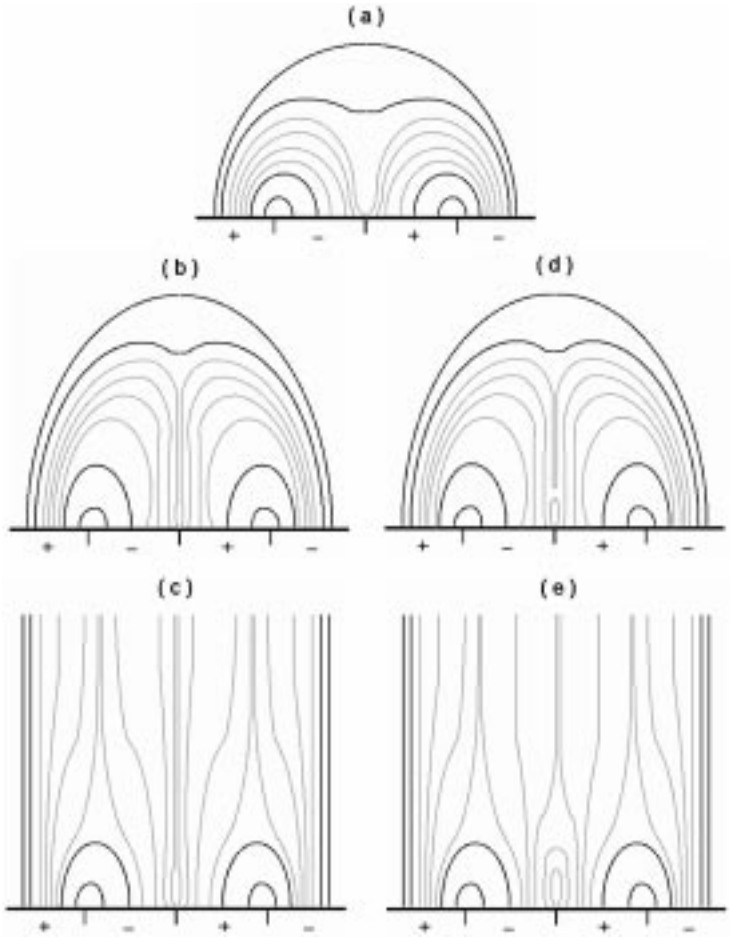

Figure 7. (a) is a simplified magnetic configuration having a bald patch. Assuming that a photospheric shear is applied around the bald patch: (b) and (c) are the expected ideal MHD evolution of the magnetic field, showing the inflation of the field lines as well as vertical current sheet formation. (d) and (e) are the expected resistive evolution of the magnetic field, showing the change of the topology of the field after the reconnection in the current sheet.

$$E_{\mathrm{mag}}(\text{partially open state}) < E_{\mathrm{mag}}(\text{sheared configuration})\ . \tag{7}$$

This point is the main hypothesis of the proposed scenario in this paper, and it should be tested numerically. Assuming that this condition is satisfied, the magnetic configuration will evolve as follows: Figure 7(a $\rightarrow$ b $\rightarrow$ d $\rightarrow$ e).

5. Interpretation of the Event

The evolution discussed in the previous section can be summarized as (i) the field near the BP is sufficiently stretched by a large shear, so that it gets a lot of energy,

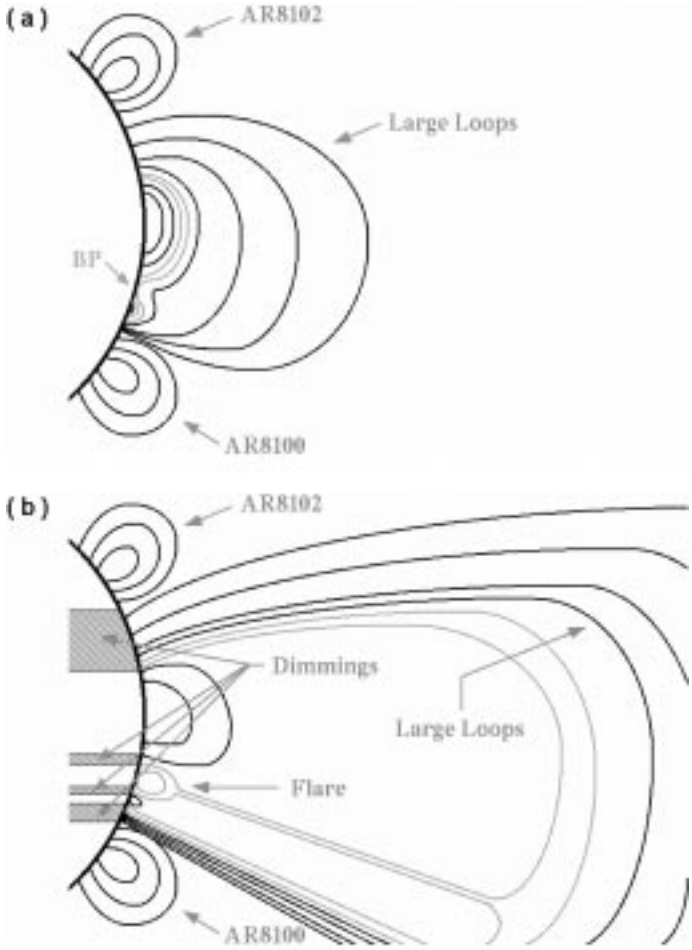

Figure 8. Sketch of the evolution of the field lines, projected at the limb.

(ii) reconnection occurs in the vertical current sheet (leading to a flare), then it triggers (iii) a loss of equilibrium which allows the field to partially open up very quickly (leading to a CME).

This scenario can be applied to the particular event studied in this paper. Figure 8(a) gives a simplified 2.5-D configuration which reproduces the main features common to the observations and the potential extrapolation (see Figures 4 and 5). Figure 8(b) shows the configuration during the process of the opening of the field. Many observed features can be reproduced from this physical sketch:

(1) The sheared field lines around the BP have formed a vertical current sheet, in which reconnection has occurred, forming new low lying loops and new large scale ones. We interpret this energy release as the observed flare and its 'F' brightening along the separatrix (see Figure 4). Maia *et al.* (1999) concluded that the time history of the individual radio burst of the 6 November 1997 CME is due to the

propagation of electrons, from AR 8100 to a region located between AR 8100 and AR 8102, along some field lines. The location of the footpoints of these field lines (shown as A and B″ in the Figure 8 of Maia *et al.,* 1999) are consistent with the footpoints of the BP separatrix found in our study.

(2) The sheared field lines have also widely expanded, pushing up the large scale overlaying transequatorial field lines interconnecting AR 8100 and AR 8102. This is also in accordance with the results of Maia *et al.* (1999) for the 6 November 1997 CME (see the loop II in their Figure 8). It is possible that the plasma in some of these loops undergoes a compression during this process. This can lead to a strong increase in brightness in the 195 Å passband of EIT. On the other hand, every field line may not follow this expansion but just be shaken by the opening of the other lines. Whether the loops are oscillating or opening, they may become very bright as L1, L2 and L3 (see Figures 3 and 4).

(3) The sudden opening of the field lines which were initially closed and near the BP separatrix may lead to a compression of the plasma at their footpoints for a short time. This is because they were initially very bent toward the photosphere, and then they quickly become vertical with the opening. This could be the explanation of the 'bright front' which appears at the northern edge of the separatrix (see Figure 4) at 10:31 UT and which has disappeared at 11:07 UT.

(4) The expansion of the field lines leads to the formation of 'open field regions' at their footpoints. In these regions, the density dramatically decreases as the loop length increases toward infinity (the open state). As a consequence the EIT 195 Å emission should become very weak in the associated regions. So the 'open field regions' naturally give dimmings (see Figure 8(b)). The one, which the scenario and the geometry of the system predict to appear in the northern hemisphere (south to AR 8102), is very wide and it is indeed observed in the EIT difference images (see Figure 3). The other predicted ones may not be observed because they are expected to be very small and dominated by the strong emission of the flare and of the loops of AR 8100.

(5) The opening of some of the large loops connecting AR 8100 and AR 8102 occurs on a significant fraction of the solar surface, typically the distance between both ARs. A projection on the limb (Figure 5) shows that it corresponds to an angular width of 50 deg for the CME. Assuming that the CME originating from AR 8100 on 6 November 1997 was created by the same process as the one we study in this paper, the angular width expected from our scenario is consistent with the SOHO/LASCO observations reported in Maia *et al.* (1999) and Delannée, Delaboudinière, and Lamy (2000). Moreover, whatever is the nature of the eruptive flare near P3 (bald patch flare, magnetic breakout or tether cutting?) our scenario involving the opening of transequatorial loops naturally explains that the flare occurs at high latitudes, while the CME itself seems to be centered on the equator, in accordance with statistical studies (see Hundhausen, 1993, and the review of Howard *et al.*, 1999).

6. Discussion

6.1. The extrapolation and the scenario

The validity of the extrapolation presented in this paper may be argued on several issues. As mentioned in Sections 2.4, 3.4, and 3.5, the use of cartesian geometry not only reduces the validity of the calculations on such a large portion of the Sun ($1641'' \times 1522''$), but also limits the comparison between observed loops and computed field lines (e.g., L2 and L3). However, Figures 4 and 5 show that the general connectivities and shapes of the transequatorial field lines follow the tendency of the observed features. As a test, we have performed similar extrapolations, but with the MDI magnetogram centered in a much larger $B = 0$ region of $3000'' \times 3000''$ to allow the field to expand freely in a 3-D volume as it could do in a spherical geometry. The computed transequatorial field lines were very similar to the ones shown on Figure 4, for the computation in the $1660'' \times 1660''$ box. Finally in an independent study, Fárník, Karlický, and Švestka (1999) found that transequatorial loops predicted by Cartesian extrapolations are present in coronal observations, demonstrating that they are not an artifact of the choice of the coordinate system.

Another issue concerns the presence of the bald patch (BP). As mentioned in Section 3.5, several extrapolations were performed in linear force-free field ($\alpha \neq 0$ and $=$ constant) with more grid points, on a smaller portions of the magnetogram centered on AR 8100. The BP was also found in the vicinity of P3. But the scenario proposed in Section 5 requires that the magnetic field is locally stressed/sheared near the BP. This may suppress the BP topology, but Titov, Priest, and Démoulin (1993) have shown that BPs are more and more likely to be present in more and more sheared configurations. We believe that the choice of Cartesian coordinates is not a issue concerning the existence and location of the BP. As the BP is due to the presence of a parasitic polarity in a surrounding field which is nearly parallel to the photosphere, and as these two conditions will be true in spherical coordinates also, the BP should not be very influenced by the choice of geometry.

The scenario proposed for the interpretation of the event also raises some questions. As mentioned in Section 4.3, the analogy with the tether-cutting model (Mikić and Linker, 1994) suggests that the evolution from Figure 7(b–e) is energetically favorable, but this should be tested through MHD simulations. Moreover, passing to 3-D may change the results expected in 2.5-D and presented on Figure 8. This has been investigated by Amari *et al.* (1996b). The first effect is that the field may not be 'sheared' at the BP, but rather 'twisted', and the second effect is that during the process of opening of the twisted field, some of the unstressed overlaying field lines (i.e., the large loops connecting AR 8100 and AR 8102) may slip sidewards. The latter will affect the amount of flux which opens during one event, reducing the size of the open field regions (i.e., of the dimming region), but we are presently unable to evaluate the importance of this effect.

6.2. RECURRENT CMES DURING 1–6 NOVEMBER 1997

During the 6 days under study in Delannée, Delaboudinière, and Lamy (2000) AR 8100 is at the origin of 8 CMEs. On these, only one is identified with its origin near the P4 polarity and the origin of the one produced on 6 November 1997 is not possible to determine. So, 6 CMEs are produced in 4 days near P3 in AR 8100. How can this recurrence be explained?

Assuming that the scenario described in Section 5 and 6 is valid, the connectivity of the magnetic field is changed after the reconnection. The new quadrupolar configuration presents one null point, so it may produce other flares as the shear still increases in the active region. The nature of these flares (confined or eruptive) will mainly depend on the amount of shear. As a new null point has been formed in the corona, a weak shear will only trigger some reconnection (as in Karpen *et al.*, 1998) while a strong shear will allow a magnetic breakout (as in Antiochos, DeVore, and Klimchuk, 1999). In the case of such an eruptive flare, the overlying transequatorial loops will open in the same way than they did in the case of the BP flare. Another possibility is that only one portion of the BP erupts during each of the CMEs, allowing other portions to erupt later. This hypothesis is supported by the fact that only the western loops inside the BP separatrix are bright during the flare (see the F feature in Figure 1(a)). Finally, the active region evolves during these five days: P4 nearly disappears and the magnetic flux of P3 increases. So, the BP length may increase as well, which re-enforces again the possibility of successive reconnections in different parts of the BP.

Figure 5 presents the observation of the loops at the limb on 8 November 1997. At this time, the 8 CMEs occurred already and one of these, on 6 November 1997, was an especially energetic one. Some observed coronal features present in the northern edge of AR 8100 seem to be open. The loops lying on the side of these features are slightly bent toward the lower altitudes. These open features support the hypothesis that the CMEs are related to the opening of the magnetic field lines. However, some of the field lines connecting AR 8100 and AR 8102 remain, so all the transequatorial loops were only partially opened by the CMEs.

The time history of the radio burst on 6 November 1997 (Maia *et al.*, 1999) shows that the first loop interaction in a region located near the BP leads to the propagation of electrons along the field lines toward a region located near the northern footpoint of the separatrix. Then a region located in AR 8102 shows some radio activity. Finally, a region located at the footpoints of the streamer show some radio activity. The time resolution of the Nançay radioheliograph is about one second. As explained in Section 5, many of these radio features observed on 6 November 1997 are consistent with our interpretation of the 3 November 1997 event. We believe that the scenario of a BP flare leading to the opening of the upper transequatorial field lines is also valid for the 6 November 1997 CME.

This consistency between the different events supports the idea that all the CMEs which have their origin near the P3 polarity in AR 8100, and which occur during 1–6 November 1997 are not only recurrent, but also might be homologous.

6.3. 'EIT WAVES' REVISITED

We have explained in Section 3.2 that the bright front observed at 10:31 UT (Figure 3(a)) and at 10:48 UT (Figure 3(b)) is very unlikely to be two different wave fronts emitted at two different times. Thus, as this bright front is observed at the same location at both times, its nature is hardly compatible with the propagation of a wave! Another interpretation of this stationary bright front may be the compression of the plasma near the footpoints of opening field lines located close to the separatrix. Figures 4(a) and 6 show that before the eruption, these field lines are very low in altitude, and bent toward the photosphere. It is reasonable to believe that when they suffer the fast opening, they suddenly become more or less vertical. This may lead to a compression of the plasma along the opening field lines. Thus, the bright front may be due to an increase in density or/and in temperature of the region. The relaxation to a stable state of the plasma in the region of compression may imply a time-scale in ranges 17–34 min as the bright front disappears between the second and the third image showing the event. However, one may remark that the bright front is much larger in the WE direction than the separatrix is, but the expansion of the field lines during the opening implies the inflation of the structure formed by these loops in the plane of the sky.

The bright front on 3 November 1997 does not seem to propagate, but our interpretation of its formation does not exclude the motion of such a structure in different cases. We believe this strongly depends on the geometry of the surrounding magnetic fields. In the most general case, the bright front is expected to propagate as the field opens further and further from the flare site. But we predict that there is no propagation (or that it is halted !) when the bright front encounters regions where the magnetic field is more or less vertical (but not necessarily open), such as at the footpoints of very large loops (transequatorial or originating from isolated active regions) or in (polar) coronal holes.

We would like here to make a remark about the production of the so called 'EIT waves' by an energy release in an explosive event. On 3 November 1997, 50 flares produced in AR 8100 are reported in *Solar Geophysical Data* report. Two of them are M class flares, which are the most intense flares produced on that day. Only 3 of the 50 flares are related to an 'EIT wave' (bright front). All of these 'EIT waves' are associated with both a dimming and a CME (Delannée, Delaboudinière, and Lamy, 2000). One of the 3 flares which are related to the 'EIT waves' is an M class flare. So, a flare is not systematically related to an 'EIT wave', even a highly energetic flare. Moreover a small energetic flare can be associated to an 'EIT wave'. This means that only the presence of a flare, whatever its energy, is not a sufficient condition for a 'EIT wave' to occur! It is worth keeping in mind that in all of

the above cases, the observed 'EIT wave' was systematically associated to a flare occurring in an active region. Other 'EIT waves' may then be observed in different environments.

Finally, all of these results tend to confirm the hypothesis that another process than a 'piston-driven wave' produced by the energy release in a flare must be involved in the production of an 'EIT wave'. Here, one can find our reason for using the term 'bright front' instead of 'EIT wave' in all this paper. We have proposed in Section 5 that the opening of the magnetic field lines can create this bright front.

7. Summary

On 3 November 1997 at 10:31 UT a flare was produced in the vicinity of the parasitic polarity P3 at the edge of the main polarity N1 of AR 8100. A bright front (or 'EIT wave') related to this flare remained between AR 8100 and AR 8102 at the same place for at least 17 min. Dimmings in intensity located between the AR 8102 and the bright front developed just after the flare. Three transequatorial loops connecting the two active regions became bright during the event. All of these phenomenon were related to a halo coronal mass ejection (CME).

We performed a potential extrapolation of a magnetogram of the region involved in this event. We found that the magnetic field lines were well correlated with the morphology of the observed transequatorial loops. We also identified a bald patch (i.e., the photospheric curve made of field lines tangential to the photosphere) at the edge of the polarity P3. The separatrix formed by the field lines passing through the bald patch (or BP) was related to an elongated brightening associated with the observed flare.

We propose the following scenario, in order to link all the observed features during the event: if a magnetic shear is applied around the BP by photospheric motions or magnetic field emergence, the following inflation of the field lines around the BP may lead to the appearance of a vertical current sheet, forming a null point in the corona through reconnection. Then subsequent reconnection at this null may redistribute the field toward a lower energy state, in a way that the reconnected field lines undergo a fast opening. The latter may then push up, and then open, the overlying transequatorial loops which are connecting the two active regions.

At the footpoints of the open field lines, the expansion of the plasma will probably lead to a dimming. The scenario we have proposed predicts that three dimmings should occur. But as the location of two of them is expected to be very close to AR 8100 and the flare (which is very bright), only the one near AR 8102 is indeed observed. In order to explain the static bright front, we have finally proposed that the fast opening of the field lines which are very close to the separatrix of the BP may lead to the compression and the heating of the plasma near their footpoints.

This suggests that a bright front can appear and remain for some time, until the plasma reaches again its stable thermodynamical state.

From the theoretical point of view, these processes will occur if the energy of the configuration of the sheared BP, overlaid by large scale closed field lines, is larger than the energy of the configuration formed by reconnection and by the opening of the large scale field lines. The demonstration of this complicated process needs MHD numerical simulations. In a first step, a 2.5-D simulation would show if the process is possible. This will be the object of a future paper.

Acknowledgements

The authors would like to thank S. Antiochos, P. Démoulin and J. Klimchuk for very stimulating discussions. The work of G.A. is funded by NASA and ONR.

References

Alissandrakis, C. E.: 1981, *Astron. Astrophys.* **100**, 197.
Aly, J.-J., and Amari, T.: 1997, *Astron. Astrophys.* **319**, 699.
Amari, T., Luciani, J.-F., Aly, J.-J., and Tagger, M.: 1996a, *Astrophys. J.* **306**, 913.
Amari, T., Luciani, J.-F., Aly, J.-J., and Tagger, M.: 1996b, *Astrophys. J.* **446**, L39.
Antiochos, S. K.: 1987, *Mem. Soc. Astron. It.* **61**, 369.
Antiochos, S. K., DeVore, C. R, and Klimchuk, J. A.: 1999, *Astrophys. J.* **510**, 485.
Aulanier, G., and Démoulin, P.: 1998, *Astron. Astrophys.* **329**, 1125.
Aulanier, G., Démoulin, P., Schmieder, B., Fang, C., and Tang, Y. H.: 1998a, *Solar Phys.* **183**, 369.
Aulanier, G., Schmieder, B., Démoulin, P., van Driel-Gesztelyi, L., and DeForest, C.: 1998b, *ASP Conf. Series* **155**, 105.
Billinghurst, M. N., Craig, I. J. D., and Sneyd, A. D.: 1993, *Astron. Astrophys.* **279**, 589.
Brueckner, G. E., Howard, R. A., Koomen, M., Korendyke, C. M., and Michels, D. J. *et al.*: 1995, *Solar Phys.* **162**, 357.
Bumba, V., Garcia, A., and Jordan, S.: 1998, *Astron. Astrophys.* **329**, 1138.
Bungey, T. N., Titov, V. S., and Priest, E. R.: 1996, *Astron. Astrophys.* **308**, 223.
Delaboudinière, J.-P., Artzner, G. E., Brunaud J., Gabriel A. H., Hochedez J. F. *et al.*: 1995, *Solar Phys* **162**, 291.
Delannée, C., Delaboudinière, J.-P., and Lamy, P.: 2000, *Astron. Astrophys.* **355**, 725.
Démoulin, P., Bagalá, L. G., Mandrini, C. H., Hénoux, J.-C., and Rovira, M. G.: 1997, *Astron. Astrophys.* **325**, 305.
Dere, K. P., Brueckner, G. E., Howard, R. A., Koomen, M. J., and Korendyke, C. M: 1997, *Solar Phys.* **175**, 601.
Fárník, F., Karlický, M., and Švestka, Z.: 1999, *Solar Phys.* **187**, 33.
Gary, G. A. and Hagyard, M. J.: 1990, *Solar Phys.* **126**, 21.
Gopalswamy, N. and Hanaoka, Y.: 1998, *Astrophys. J.* **498**, 179.
Gopalswamy, N., Hanaoka, Y., Kosugi, T., Lepping, R., *et al.*: 1998, *Geophys. Res. Letters* **25**, 2485.
Harrison, R. A.: 1986, *Astron. Astrophys.* **162**, 283.
Howard, R. A., Dere, K. P., Moses, D., Plunkett, S. P., St. Cyr, O. C., and Sheeley, N. R.: 1999, Proceedings of the SOHO8 Meeting, *ESA SP* **446**, in press.
Hudson, H. S.: 1997, *23rd Meeting of the IAU*, 26–27 August 1997, Kyoto, Japan, 19.

Hudson, H. S., Acton, L. W., and Freeland, S. L.: 1996, *Astrophys. J.* **470**, 629.
Hundhausen, A.: 1993, *J. Geophys. Res.* **98**, 13,177.
Innes, D. E., Inhester, B., Srivastava, N., Brekke, P., Harrison, R. A. *et al.*: 1999, *Solar Phys.* **186**, 337.
Karpen, J. T., Antiochos, S. K., and DeVore, C. R.: 1990, *Astrophys. J.* **356**, L67.
Karpen, J. T., Antiochos, S. K., and DeVore, C. R.: 1991, *Astrophys. J.* **382**, 327.
Karpen, J. T., Antiochos, S. K., DeVore, C. R., and Golub, L.: 1998, *Astrophys. J.* **495**, 491.
Khan, J. I., and Hudson, H. S.: 1999, *Geophys. Res. Letters*, submitted.
Kocharov, L., Lee, J., Zirin, H., Kovaltsov, G., Usoskin, I. *et al.*: 1994, *Solar Phys.* **155**, 149.
Krucker, S., Larson, D., Lin, R., and Thompson, B.: 1999, *Astrophys. J.* **519**, 864.
Low, B. C. and Wolfson, R.: 1988, *Astrophys. J.* **324**, 574.
Maia, D., Voulidas, A., Pick, M., Howard, R., Schwenn, R., and Magalhães, A.: 1999, *J. Geophys. Res.* **104** (A6), 12 507.
Mikić, Z., and Linker, J. A.: 1994, *Astrophys. J.* **430**, 898.
Moreton, G. E.: 1961, *Sky Telesc.* **21**, 145.
Nakajima, H., Kawashima, S., Shinohara, N., Shjomi, Y., and Enome, S.: 1990, *Astrophys. J. Suppl.* **73**, 177.
Ramsey, H. E. and Smith, S. F.: 1966, *Astrophys. J.* **71**, 197.
Reigler, G., Ling, J., Mahoney, W., Prince, T., Wheaton, W., Willett, J., Zirin, H, and Jacobson, A.: 1982, *Astrophys. J.* **259**, 392.
Rust, D. M. and Hildner, E.: 1976, *Solar Phys.* **48**, 381.
Scherrer, P. H., Bogart, R. S., Bush, R. I., Hoeksema, J. T., Kosovichev, A. G. *et al.*: 1995, *Solar Phys.* **162**, 129.
Schmieder, B., Démoulin, P., Aulanier G., and Golub, L.: 1996, *Astrophys. J.* **467**, 881.
Seehafer, N.: 1986, *Solar Phys.* **105**, 223.
Seehafer, N.: 1985, *Solar Phys.* **96**, 307.
Seehafer, N. and Staude, J.: 1980, *Solar Phys.* **67**, 121.
Sterling, A. C. and Hudson, H. S.: 1997, *Astrophys. J.* **491**, 55.
Sturrock, P. A.: 1989, *Solar Phys.* **121**, 387.
Titov, V. S., Priest, E. R., and Démoulin, P.: 1993, *Astron. Astrophys.* **276**, 564.
Titov, V. S. and Démoulin, P.: 1999, *Astron. Astrophys.* in press.
Thompson, B. J., Plunkett, S. P., Gurman, J. B., Newmark, J. S., St. Cyr, O. C., and Michels, D. J.: 1998, *Geophys. Res. Letters* **25**, 2465.
Thompson, B. J., Gurman, B., Neupert, W., Newmark, J. *et al.*: 1999, *Astrophys. J.* **517**, 151.
Torsti, J., Kocharov, L., Teittinen, M., and Thompson, B.: 1999, *Astrophys. J.* **510**, 460.
Uchida, Y.: 1970, *Publ. Astron. Soc. Japan* **22**, 341.
Vekstein, G. E., Priest, E. R., and Amari, T.: 1991, *Astron. Astrophys.* **243**, 492.
Vernazza, J. E., Avrett, E. H., and Loeser, R.: 1981, *Astrophys. J. Suppl.* **45**, 635.
Wills-Davey, M. J. and Thompson, B. J.: 1999, *Solar Phys.* **190**, 459 (this issue).
Yokoyama, T. and Shibata, K.: 1995, *Nature* **375**, 42.